Hindawi Publishing Corporation
EURASIP Journal on Image and Video Processing
Volume 2008, Article ID 487618, 9 pages
doi:10.1155/2008/487618

Research Article

Quantification and Standardized Description of Color Vision Deficiency Caused by Anomalous Trichromats—Part I: Simulation and Measurement

Seungji Yang,[1] Yong Man Ro,[1] Edward K. Wong,[2] and Jin-Hak Lee[3]

[1] *Image and Video Systems Lab, Information and Communications University, Munji 119, Yuseong, Daejeon 305-732, South Korea*
[2] *Department of Ophthalmology, University of California at Irvine, Irvine, CA 92697-4375, USA*
[3] *Department of Ophthalmology, Seoul National University Hospital, 28 Yongon-Dong, Chongno-Gu, Seoul 110-744, South Korea*

Correspondence should be addressed to Yong Man Ro, yro@icu.ac.kr

Received 8 October 2007; Revised 14 December 2007; Accepted 22 December 2007

Recommended by Alain Tremeau

The MPEG-21 Multimedia Framework allows visually impaired users to have an improved access to visual content by enabling content adaptation techniques such as color compensation. However, one important issue is the method to create and interpret the standardized CVD descriptions when making the use of generic color vision tests. In Part I of our study to tackle the issue, we present a novel computerized hue test (CHT) to examine and quantify CVD, which allows reproducing and manipulating test colors for the purposes of computer simulation and analysis of CVD. Both objective evaluation via color difference measurement and subjective evaluation via clinical experiment showed that the CHT works well as a color vision test: it is highly correlated with the Farnsworth-Munsell 100 Hue (FM100H) test and allows for a more elaborate and correct color reproduction than the FM100H test.

1. INTRODUCTION

Today, the use of color display in the multimedia-enabled devices is very common. Portable multimedia devices even allow real-time displays of high-quality color information. As such, with the proliferation of color displays, it becomes more important for ordinary people to perceive colors correctly. Color displays create no problems for normal people, although color perception might be slightly different among different people with a different normal color vision. Meanwhile, color displays do cause problems for people with color vision deficiency (CVD). For these people, the use of rich colors may lead to confusion. It may even result in misinterpreting information that colors are carrying because people with CVD may suffer from inability to discriminate among different colors. The problem even gets worse in cases where color is the only visual clue to recognize something important.

Up to 8% of the world's male population exhibits a type of CVD. More than 80% of them has one form of anomalous trichromacy, which demonstrates a milder and variable severity than those with dichromacy [1]. It is known that there is no satisfactory cure for CVD and this condition is lifelong. However, there has been a little consideration about any assistance to people with CVD in color perception.

Recently, universal multimedia access (UMA) has become an emerging trend in the world of multimedia communication. A UMA system adapts rich multimedia content to various constraints imposed by users, devices, and networks, providing the best possible multimedia experience to a particular user, anytime and anywhere. Meanwhile, the recently developed MPEG-21 multimedia framework facilitates the realization of UMA systems in an interoperable manner [2]. Among other tools that enable seamless access to multimedia, the MPEG-21 multimedia framework provides a normative description of CVD. In this way, visually impaired users can have improved access to visual content through content adaptation, more specifically by means of color compensation. In this context, the color compensation process can be guided and optimized by the CVD description standardized by the MPEG-21 [2, 3].

However, to suitably accommodate color compensation using the CVD description provided by the MPEG-21

multimedia framework, two important issues should be resolved. The first issue consists of matching CVD characteristics to the MPEG-21 CVD description, while the second issue consists of the design of a content adaptation scheme that is harmonized with the MPEG-21 CVD description. In this paper, in order to tackle these two issues, we present a comprehensive study that examines CVD through a computerized color vision test (referred to as CHT), utilizes color compensation techniques through anomalous cone modeling, and quantifies color vision defects using a new computerized hue test (CHT) with color compensation.

The major contribution of Part I of our study is the development of a reproducible, computer-based color vision test, called the CHT. The fundamental idea behind the CHT stems from generic color arrangement tests such as the Farnsworth-Munsell 100-Hue (referred to as FM100H) test. One major difference is the fact that the CHT is a reproducible and computer-based test, which allows easy manipulation of test colors for the purposes of simulation and analysis of anomalies in color vision. In Part I of our study, we have also compared the efficiency of the CHT to the FM100H test. A computer simulation is used to study the variation of color defects according to the spectral cone shift. Finally, in Part II of our study, we will discuss a color compensation scheme for anomalous trichromats. This color compensation scheme operates according to the deficiency degree standardized by the MPEG-21 multimedia framework.

2. RELATED WORK: CONVENTIONAL COLOR VISION TESTS

In order to examine anomalies in color vision, many clinical color vision tests were developed several decades ago. In general, two major test methodologies have been developed: one is related to the colors reflected from a colored object, while the other is related to the colors emitted from a solid light source. The tests using reflected light are subdivided into two types: one type is the pseudoisochromatic plate tests such as the Ishihara test [4, 5] and the Hardy-Rand-Rittler (HRR) test [6], while the other type is the color arrangement testing such as the Farnsworth Panel D-15 test and the FM100H test [7–9]. The test using emitted colors includes several types of anomaloscopes developed by Jyrki [10].

Among all of the tests, the FM100H test is known to be one of the most accurate tests showing high sensitivity to find color defects at an early stage and to determine the degrees of severity. The FM100H test has the subject place 85 different color caps in a specific order. The color caps are divided into four groups, each of which comprises 22, 21, 21, and 21 color caps, respectively. The type of CVD and its severity degree are determined by the location of the caps after testing. This would demonstrate the confusion of the subject's color perception and the total error score of the caps arranged by the subject according to the hue [11, 12].

However, it takes a long time to perform the FM100H test. An analysis of the results is difficult when testing a large number of subjects. In addition, lighting conditions can affect the test results unless these conditions are carefully controlled to give a fixed and stable radiation. The color caps can be discolored or changed due to contamination over time. Due to these problems, although the FM100H test is known to be the most accurate clinical test, it has been less commonly used than many other tests.

Several studies have been done to simplify the analysis of the results of the FM100H test [6, 11, 13]. In this study, we present an alternative approach by considering a computerized color vision test. Color vision testing using the computer has a number of important advantages. In using the computer and monitor after calibration, any color can be easily reproduced as well as changed for specific purposes. The test and resulting data can be easily managed, analyzed, and shared. Modifications and improvements of the test method are also possible if necessary.

3. COMPUTERIZED HUE TEST FOR COLOR VISION DEFICIENCY

3.1. Color vision deficiency

A significant number of studies have been conducted to understand human color perception and cone fundamentals [14–20]. Normal color vision has three cones whose peak sensitivities lie in the long-wavelength (L), middle-wavelength (M), and short-wavelength (S) bands of the visible spectrum [1, 19]. Meanwhile, CVD arises from two causes: (1) complete lack of a cone pigment or (2) alteration of one of the three cone pigments. The former is known as dichromacy, and the latter is known as anomalous trichromacy. There is an extreme case, called achromatopsia, where no cone is present in the eyes. Anomalous trichromacy is known to have various causes [1]. The most frequent one is the shifting of cone spectral sensitivity from the normal position [1, 15, 17, 21]. Anomalous trichromats have three classes of cone pigments, but the peak sensitivity wavelengths of two of these classes lie closer together. Depending on the type of shifted cone, anomalous trichromacy is divided into protanomalous (having a shifted L cone), deuteranomalous (having a shifted M cone), and tritanomalous (having a shifted S cone) trichromacy. The protanomalous and deuteranomalous trichromats are X-chromosome-linked, genetic, anomalous trichromats, while the tritanomalous trichromats are mostly acquired. Due to abnormal cone characteristics, people with CVD may have great difficulty with color discrimination.

3.2. Implementation of the computerized hue test

The CHT is a kind of color arrangement test. It is designed to display several color caps with different colors on a black background on the monitor. The subject arranges the randomized color caps in order of hue. Thereby, the color stimulus arrays of the CHT resemble those of the conventional FM100H test. They consist of 85 color caps that are ranked according to the perceptual difference between adjacent colors.

In order to ensure uniform color differences in visual perception, the HSV (hue-saturation-value) color space is employed. The HSV space allows dividing a stimulus into two

chromatic components of H (hue) and S (saturation), and one achromatic component, that is luminance, of V (value). The S and V parameter values have the range of 0 to 1, and the H parameter has the range of 0° to 360°.

In the CHT, only the hue value is variable while luminance and saturation values are fixed [15–18]. The saturation of the color caps is 0.24, the value of the color caps is 0.58, and the luminance of the background is 0 (zero). The angular size of a color cap is 1°, where color caps on the monitor are displayed at 60 cm (normal arms length) away from the subject's eye. This is analogous to that of the FM100H test. The difference of the hue values of any two adjacent colors is the same for all color caps. To facilitate the subject's concentration on testing, the whole test procedure is divided into four short steps: 22 color caps with hue values from 0° to 90° in the first step, 21 color caps with hue values from 90° to 180° in the second step, 21 color caps with hue values from 180° to 270° in the third step, and 21 color caps with hue values from 270° to 360° in the fourth step.

The CHT is performed on a computer display monitor. As such, color vision testing through a display device is dependent on visual characteristics of individuals as well as spectral characteristics of the display device. Different display devices often produce different characteristics of the same color. Thus, an important requirement for computerized color vision testing is that the test monitor should be calibrated before each test. The CHT must be performed on a calibrated monitor device.

The severity degree of color deficiency is quantitatively measured by using the total error score (TES), which is analogous to conventional FM100H testing. The TES is a measure of the accuracy of a subject in arranging the color caps to form a gradual transition in hue between the two anchor caps. A high number of misplacements result in a large TES [1].

3.3. Anomalous color vision simulation on the computerized hue test

A monitor device has its own spectral characteristics. The color that one perceives is different according to the spectral characteristics of the monitor. In this section, we simulate colors emitted from the monitor especially in the anomalous trichromacy point of view. The computer simulation of dichromacy color perception was developed by Brettel et al. [22], Vienot and Brettel [23], and Rigden [24]. However, there has been no literature about the simulation of anomalous color perception. In this paper, we develop the computer simulation of the anomalous color spectra. Furthermore, the simulation of anomalous color spectra is utilized to develop the color compensation method.

Given the CHT, we expect that anomalous trichromats will produce a lower score than do normal trichromats. To objectively measure the visual difference among caps of the CHT, anomalous color vision is visualized on the CHT by projecting stimuli of all the color caps into the visual perception of anomalous trichromacy. This process is referred to as simulation. In order to do so, let us first define c_i to be the ith color cap of the CHT. This can also be written as $c_i = \{h_i, s_i, v_i\}$. Then, a set of the 85 color caps, denoted as $\mathbf{C}$, can be written as follows:

$$\mathbf{C} = \{c_1, c_2, c_3, \ldots, c_{85}\}, \tag{1}$$

where the hue difference between any adjacent two color caps is approximately 4° (= 360°/85), and where saturation and luminance values are the same for all color caps.

Then, each color cap in the HSV color space is converted to a corresponding cap in the RGB color space. The color cap in the RGB space is written as follows:

$$c_i = \{r_i, g_i, b_i\} = \{h_i, s_i, v_i\}. \tag{2}$$

Given a color cap in the RGB space, the simulation is performed as shown in Figure 1. First, the original color in the RGB space is projected into color in the anomalous LMS space that presents a color stimulus on the space of L, M, and S cones. This can be done by using an anomalous color transformation matrix, called $\mathbf{T}^{\text{anomalous}}$ that can be specified to $\mathbf{T}^{\text{protan}}$ and $\mathbf{T}^{\text{deutan}}$ for protanomalous and deuteranomalous, respectively. Next, the color in the anomalous LMS space is converted back to any defective color in the RGB color space by using a normal color transformation matrix called $\mathbf{T}^{\text{normal}}$. The resulting color shows how the original color is perceived by a particular anomalous trichromat.

In order to calculate $\mathbf{T}^{\text{normal}}$, the spectral sensitivity of normal L, M, and S cones regarding color emitted from RGB phosphors in a color monitor can be defined as

$$\begin{aligned}
L_R^{\text{normal}} &= k_L \int E_R(\lambda) L(\lambda) d\lambda, \\
L_G^{\text{normal}} &= k_L \int E_G(\lambda) L(\lambda) d\lambda, \\
L_B^{\text{normal}} &= k_L \int E_B(\lambda) L(\lambda) d\lambda, \\
M_R^{\text{normal}} &= k_M \int E_R(\lambda) M(\lambda) d\lambda, \\
M_G^{\text{normal}} &= k_M \int E_G(\lambda) M(\lambda) d\lambda, \\
M_B^{\text{normal}} &= k_M \int E_B(\lambda) M(\lambda) d\lambda, \\
S_R^{\text{normal}} &= k_S \int E_R(\lambda) S(\lambda) d\lambda, \\
S_G^{\text{normal}} &= k_S \int E_G(\lambda) S(\lambda) d\lambda, \\
S_B^{\text{normal}} &= k_S \int E_B(\lambda) S(\lambda) d\lambda,
\end{aligned} \tag{3}$$

where $E_R(\lambda)$, $E_G(\lambda)$, and $E_B(\lambda)$ are R, G, and B primary emission functions of the color monitor device, respectively, and $L(\lambda)$, $M(\lambda)$, and $S(\lambda)$ are spectral L, M, and S cone response functions of the normal subject, respectively. The color monitor is assumed to be calibrated, thus having ideal emission functions so that the neutral point of the LMS cone response is purely white. Then, we can compute the k of the parameters such that the following condition is satisfied: $\sum L = \sum M = \sum S = 1$ [25].

The $\mathbf{T}^{\text{normal}}$ means the spectral response of normal LMS cones about RGB colors. So the values from (3) comprise co-

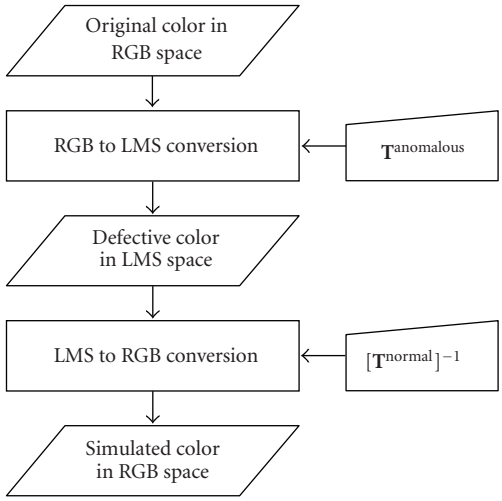

Figure 1: Procedure of anomalous color perception.

efficients for $\mathbf{T}^{\text{normal}}$ as follows:

$$\mathbf{T}^{\text{normal}} = \begin{bmatrix} L_R^{\text{normal}} & L_G^{\text{normal}} & L_B^{\text{normal}} \\ M_R^{\text{normal}} & M_G^{\text{normal}} & M_B^{\text{normal}} \\ S_R^{\text{normal}} & S_G^{\text{normal}} & S_B^{\text{normal}} \end{bmatrix}. \tag{4}$$

By using the matrix $\mathbf{T}^{\text{normal}}$, the RGB value of the ith color cap displayed through the monitor can be transformed into an LMS value as follows:

$$\begin{aligned} \begin{bmatrix} l_i \\ m_i \\ s_i \end{bmatrix} &= \mathbf{T}^{\text{normal}} \cdot \begin{bmatrix} r_i \\ g_i \\ b_i \end{bmatrix} \\ &= \begin{bmatrix} L_R^{\text{normal}} & L_G^{\text{normal}} & L_B^{\text{normal}} \\ M_R^{\text{normal}} & M_G^{\text{normal}} & M_B^{\text{normal}} \\ S_R^{\text{normal}} & S_G^{\text{normal}} & S_B^{\text{normal}} \end{bmatrix} \cdot \begin{bmatrix} r_i \\ g_i \\ b_i \end{bmatrix}. \end{aligned} \tag{5}$$

Since protanomaly is characterized by an anomalous L cone, its spectral cone sensitivity should be affected by the shift amount of the protanomalous L cone. Thus, the spectral cone response of a protanomalous L cone can be obtained by

$$\begin{aligned} L_R^{\text{protan}}(\Delta\lambda) &= k_L \int E_R(\lambda) L'(\lambda, \Delta\lambda) d\lambda, \\ L_G^{\text{protan}}(\Delta\lambda) &= k_L \int E_G(\lambda) L'(\lambda, \Delta\lambda) d\lambda, \\ L_B^{\text{protan}}(\Delta\lambda) &= k_L \int E_B(\lambda) L'(\lambda, \Delta\lambda) d\lambda, \end{aligned} \tag{6}$$

where $L'(\lambda, \Delta\lambda)$ is a protanomalous L cone shifted by $\Delta\lambda$ from the normal position.

As ever, deuteranomalous spectral cone sensitivity should be affected by the shift amount of the deuteranomalous M cone. Therefore, the spectral cone response of a deuteranomalous M cone can be obtained by

$$\begin{aligned} M_R^{\text{deutan}}(\Delta\lambda) &= k_M \int E_R(\lambda) M'(\lambda, \Delta\lambda) d\lambda, \\ M_G^{\text{deutan}}(\Delta\lambda) &= k_M \int E_G(\lambda) M'(\lambda, \Delta\lambda) d\lambda, \\ M_B^{\text{deutan}}(\Delta\lambda) &= k_M \int E_B(\lambda) M'(\lambda, \Delta\lambda) d\lambda, \end{aligned} \tag{7}$$

where $M'(\lambda, \Delta\lambda)$ is a deuteranomalous M cone shifted by $\Delta\lambda$ from the normal position.

Given the protanomalous L cone sensitivity, the conversion matrix ($\mathbf{T}^{\text{protan}}$) for the protanomaly that shows the LMS cone response of RGB colors can be defined as

$$\mathbf{T}^{\text{protan}}(\Delta\lambda) = \begin{bmatrix} L_R^{\text{protan}}(\Delta\lambda) & L_G^{\text{protan}}(\Delta\lambda) & L_B^{\text{protan}}(\Delta\lambda) \\ M_R^{\text{normal}} & M_G^{\text{normal}} & M_B^{\text{normal}} \\ S_R^{\text{normal}} & S_G^{\text{normal}} & S_B^{\text{normal}} \end{bmatrix}. \tag{8}$$

Similarly, given the deuteranomalous M cone sensitivity, the conversion matrix ($\mathbf{T}^{\text{deutan}}$) for the deuteranomaly can be defined as

$$\mathbf{T}^{\text{deutan}}(\Delta\lambda) = \begin{bmatrix} L_R^{\text{normal}} & L_G^{\text{normal}} & L_B^{\text{normal}} \\ M_R^{\text{deutan}}(\Delta\lambda) & M_G^{\text{deutan}}(\Delta\lambda) & M_B^{\text{deutan}}(\Delta\lambda) \\ S_R^{\text{normal}} & S_G^{\text{normal}} & S_B^{\text{normal}} \end{bmatrix}. \tag{9}$$

By using the $\mathbf{T}^{\text{protan}}$, the RGB value of the ith color cap is transformed to the protanomalous LMS value, referred to as $c_i^{\text{protan}} = \{l_i^{\text{protan}}, m_i, s_i\}$, as follows:

$$\begin{aligned} \begin{bmatrix} l_i^{\text{protan}} \\ m_i \\ s_i \end{bmatrix} &= \mathbf{T}^{\text{protan}}(\Delta\lambda) \cdot \begin{bmatrix} r_i \\ g_i \\ b_i \end{bmatrix} \\ &= \begin{bmatrix} L_R^{\text{protan}}(\Delta\lambda) & L_G^{\text{protan}}(\Delta\lambda) & L_B^{\text{protan}}(\Delta\lambda) \\ M_R^{\text{normal}} & M_G^{\text{normal}} & M_B^{\text{normal}} \\ S_R^{\text{normal}} & S_G^{\text{normal}} & S_B^{\text{normal}} \end{bmatrix} \cdot \begin{bmatrix} r_i \\ g_i \\ b_i \end{bmatrix}. \end{aligned} \tag{10}$$

By using the $\mathbf{T}^{\text{deutan}}$, the RGB value of the ith color cap is transformed to the deuteranomalous LMS value, referred to as $c_i^{\text{deutan}} = \{l_i, m_i^{\text{deutan}}, s_i\}$, as follows:

$$\begin{aligned} \begin{bmatrix} l_i \\ m_i^{\text{deutan}} \\ s_i \end{bmatrix} &= \mathbf{T}^{\text{deutan}}(\Delta\lambda) \cdot \begin{bmatrix} r_i \\ g_i \\ b_i \end{bmatrix} \\ &= \begin{bmatrix} L_R^{\text{normal}} & L_G^{\text{normal}} & L_B^{\text{normal}} \\ M_R^{\text{deutan}}(\Delta\lambda) & M_G^{\text{deutan}}(\Delta\lambda) & M_B^{\text{deutan}}(\Delta\lambda) \\ S_R^{\text{normal}} & S_G^{\text{normal}} & S_B^{\text{normal}} \end{bmatrix} \cdot \begin{bmatrix} r_i \\ g_i \\ b_i \end{bmatrix}. \end{aligned} \tag{11}$$

Consequently, $c_i^{\text{protan}} = \{r_i^{\text{protan}}, g_i^{\text{protan}}, b_i^{\text{protan}}\}$, the color perceived by the protanomalous, can be simulated as follows:

$$\begin{bmatrix} r_i^{\text{protan}} \\ g_i^{\text{protan}} \\ b_i^{\text{protan}} \end{bmatrix} = \begin{bmatrix} L_R^{\text{normal}} & L_G^{\text{normal}} & L_B^{\text{normal}} \\ M_R^{\text{normal}} & M_G^{\text{normal}} & M_B^{\text{normal}} \\ S_R^{\text{normal}} & S_G^{\text{normal}} & S_B^{\text{normal}} \end{bmatrix}^{-1} \cdot \begin{bmatrix} l_i^{\text{protan}} \\ m_i \\ s_i \end{bmatrix}, \tag{12}$$

where the protanomalous LMS value, $c_i^{\text{protan}} = \{l_i^{\text{protan}}, m_i, s_i\}$, is converted into any defective color in the RGB color space by using the inverse conversion matrix $[\mathbf{T}^{\text{normal}}]^{-1}$.

Consequently, $c_i^{\text{deutan}} = \{r_i^{\text{deutan}}, g_i^{\text{deutan}}, b_i^{\text{deutan}}\}$, the color perceived by the deuteranomalous, can be simulated as follows:

$$\begin{bmatrix} r_i^{\text{deutan}} \\ g_i^{\text{deutan}} \\ b_i^{\text{deutan}} \end{bmatrix} = \begin{bmatrix} L_R^{\text{normal}} & L_G^{\text{normal}} & L_B^{\text{normal}} \\ M_R^{\text{normal}} & M_G^{\text{normal}} & M_B^{\text{normal}} \\ S_R^{\text{normal}} & S_G^{\text{normal}} & S_B^{\text{normal}} \end{bmatrix}^{-1} \cdot \begin{bmatrix} l_i \\ m_i^{\text{deutan}} \\ s_i \end{bmatrix}, \tag{13}$$

where the deuteranomalous LMS value, $c_i^{\text{deutan}} = \{l_i, m_i^{\text{deutan}}, s_i\}$, is converted into any defective color in the RGB color space by using the inverse conversion matrix $[\mathbf{T}^{\text{normal}}]^{-1}$.

4. EXPERIMENT

For the experiments, colors for the test were produced on a personal computer equipped with a Matrox G550 graphics card with a fixed resolution of 1024×768 pixels and a fixed color depth of 24 bits of true colors. The test monitor (Samsung SyncMaster 950 series) has a screen refresh rate of 75 times per second. Its color temperature was approximately set to a value of $9000 \sim 9700$ K, which is equivalent to daylight color. The monitor was also adjusted to 90% of contrast and 80% of brightness in a dark room.

The experiment is composed of two parts: one is the measure of color defects by simulation of colors on the CHT in view of anomalous trichromacy, and the other is the measure of color defects by clinical testing on the CHT on the subject. From the simulation, we projected to observe defects on color discrimination according to the shift amount of the abnormal cones.

4.1. Objective measure of CVD by simulation

A computer simulation has been performed with 85 color caps in the CHT. Figure 2 illustrates the result of the simulation. Figure 2(a) depicts the gamut of color caps simulated for the protanomalous subject. The protanomalous gamut becomes much smaller than in the normal subject. It means that anomalous trichromats with a severe deficiency degree have a smaller color gamut that causes defective color perception. Likewise, Figure 2(b) depicts the gamut of color caps simulated from the view of deuteranomalous subjects. Similar to the protanomalous case, the deuteranomalous gamut becomes much smaller than in the normal subject as well.

To verify the color confusion line that arises from anomalous trichromacy, we simulate the hue values of 85 caps in the CHT. Figure 3 shows the hue simulation of anomalous trichromacy for the 85 color caps in the CHT. The hue values are normalized from 0.0 to 1.0. The main confusion lines of the protanomalous subject are approximately 0.1882 and 0.7414, while the main confusion lines of the deuteranomalous subject are approximately 0.1647 and 0.6705. From the simulation results, we see that the colors around the two confusion lines, which would be assumed to be perceived by the subjects who have an anomalous trichromacy, have little variation in hue. This means that the subjects who have an anomalous trichromacy have suffered from differentiating among colors near the confusion lines. It should also be noted that the confusion lines are broader as the shift amount of the abnormal cone increases, meaning that bigger shift amount of the abnormal cone leads to more confusion among colors around the confusion lines. These results demonstrate that computer simulation would work well.

We also measured the difference of colors between the normal cap and its simulated cap with various deficiency degrees. The color difference is an objective measure of difference between two colors in human color perception. The measured color difference represents defective color perception of the subjects who have an anomalous trichromacy. Based on the color differences, we can expect how an anomalous trichromat would suffer from differentiating between two colors. In order to measure the color difference in deficiency degree, the spectral shift of abnormal cones, which are known to have a value from 2 to 20 nm [1], has been applied. We use a popular color difference metric, the 1976 CIE $L^*a^*b^*$ color difference, where the nonlinear relationship for L^*, a^*, and b^* is intended to mimic the logarithmic response of the human eye. In order to accommodate the color difference to different spectral cone shifts, the color difference metric has been changed for the protanomalous cone shift $(\Delta\lambda)$ to the following:

$$D_i^{\text{protan}}(\Delta\lambda) = \sqrt{\left(L_i^* - L_i^{*\text{protan}}(\Delta\lambda)\right)^2 + \left(a_i^* - a_i^{*\text{protan}}(\Delta\lambda)\right)^2 + \left(b_i^* - b_i^{*\text{protan}}(\Delta\lambda)\right)^2}, \tag{14}$$

where $\{L_i^*, g_i^*, b_i^*\}$ is a $L^*a^*b^*$ value of the ith color cap that is the same as $\{r_i, g_i, b_i\}$ in the RGB space, and $\{L_i^{*\text{protan}}, a_i^{*\text{protan}}, b_i^{*\text{protan}}\}$ is a simulated $L^*a^*b^*$ value for anomalous trichromacy, which is the same as $\{r_i^{\text{protan}}, g_i^{\text{protan}}, b_i^{\text{protan}}\}$ in the RGB space.

Similarly, the color difference for deuteranomalous cone shift $(\Delta\lambda)$ is measured as

$$D_i^{\text{deutan}}(\Delta\lambda) = \sqrt{\left(L_i^* - L_i^{*\text{deutan}}(\Delta\lambda)\right)^2 + \left(a_i^* - a_i^{*\text{deutan}}(\Delta\lambda)\right)^2 + \left(b_i^* - b_i^{*\text{deutan}}(\Delta\lambda)\right)^2}, \tag{15}$$

where $\{L_i^{*\text{deutan}}, a_i^{*\text{deutan}}, b_i^{*\text{deutan}}\}$ is a simulated $L^*a^*b^*$ value for anomalous trichromacy, which is the same as $\{r_i^{\text{deutan}}, g_i^{\text{deutan}}, b_i^{\text{deutan}}\}$ in the RGB space.

Figure 4 shows the average color difference between normal caps and associated simulated caps of the CHT. It was observed that the smaller the ability of a subject to differentiate between two colors, the higher the color difference existed between the stimulations. The color difference is linearly proportional to the spectral cone shift in both protanomalous and deuteranomalous cases. This basically means, as expected, that the higher the spectral cone shift, the smaller the ability of a subject to differentiate among colors.

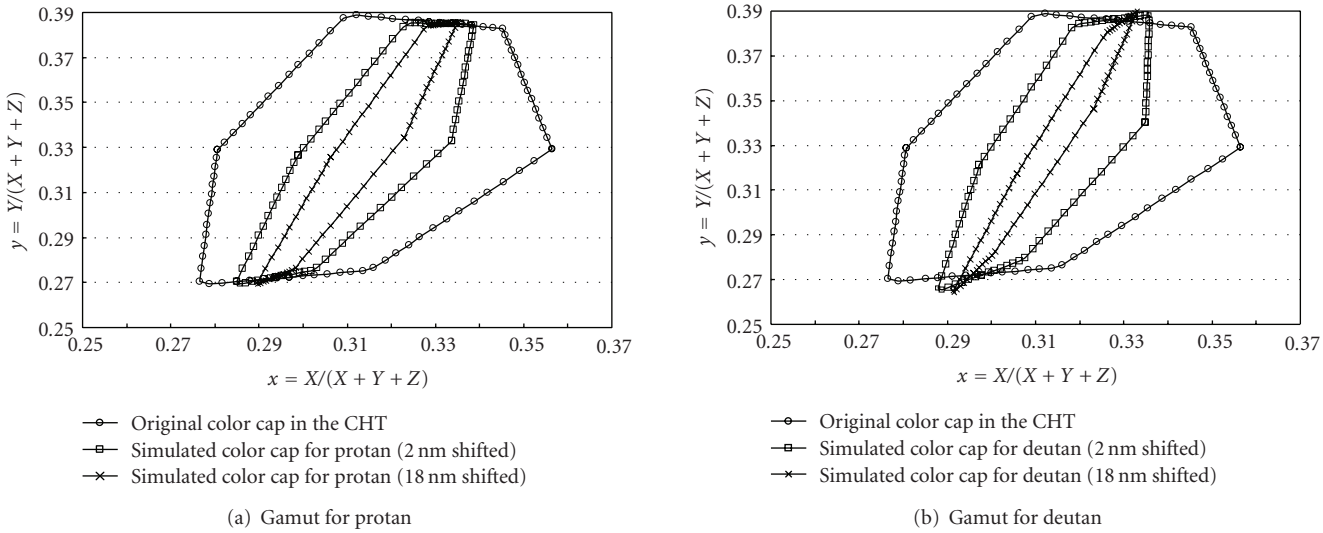

(a) Gamut for protan (b) Gamut for deutan

Figure 2: Gamut of 85 color caps of the CHT. (Note that the dots show the cap color position in x-y color space.)

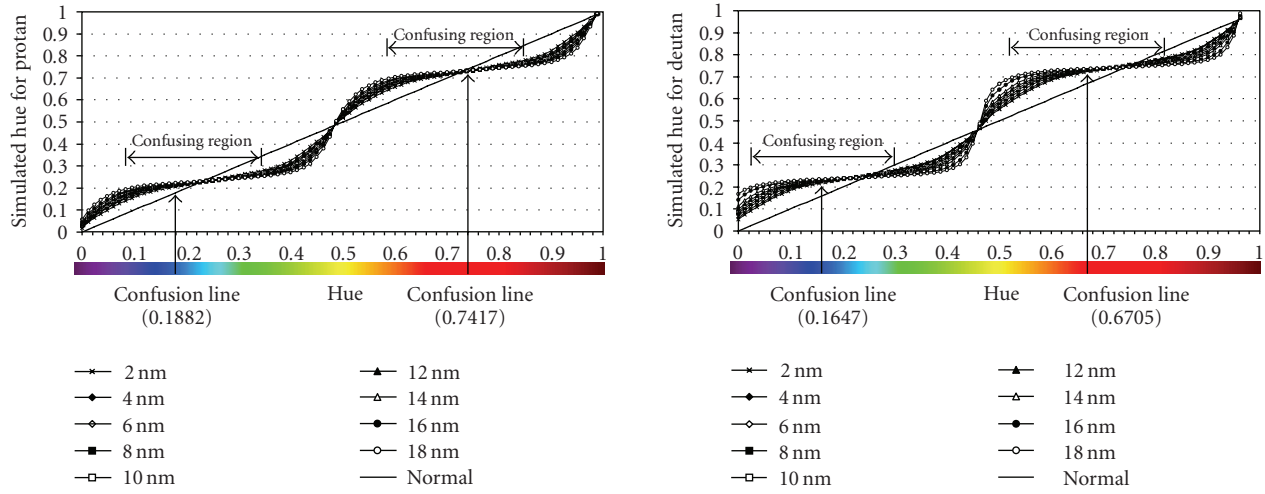

(a) Simulated hue for protan (b) Simulated hue for deutan

Figure 3: Simulated hue of anomalous trichromacy versus normal hue value for the 85 color caps in the CHT.

4.2. Subjective measure of CVD by clinical testing

In the clinical experiment on the CHT, the subject selects color caps displayed on the monitor screen and puts them in order according to hue. Given a set of ordered color caps by a subject, the TES is computed. The test time is limited to 2 minutes per test to obtain consistency in test results for all subjects. The subjects perform the test 60 cm (normal arms length) away from the monitor screen. Exclusion factors [26] that may affect color vision include the following: subjects who have central nervous system diseases, those who take medicines that may affect vision, those who have any organic ophthalmologic diseases that may influence color vision, those who are under 10 years of age, and those who cannot cooperate well in doing the test. The corrected *Snellen* visual acuities of the subjects measured better than 20/25. In all tests, the subjects were informed about the test procedure from a tester, and then they twice performed the FM100H test and CHT, repeating the original test one week later. After the TES of each test was obtained, the average according to each test method was calculated and the difference was evaluated. The reproducibility of the color vision test was determined by the coefficient of variation of the test, and the correlation between the two tests was acquired through the *Spearman* regression analysis.

The total number of subjects was 130 (43 men and 87 women), having an average age of 34 years (14–67 years of age). Among those subjects, 89 subjects were determined to be normal and 41 subjects were determined to be abnormal with the HRR test, the FM100H test, and the CHT.

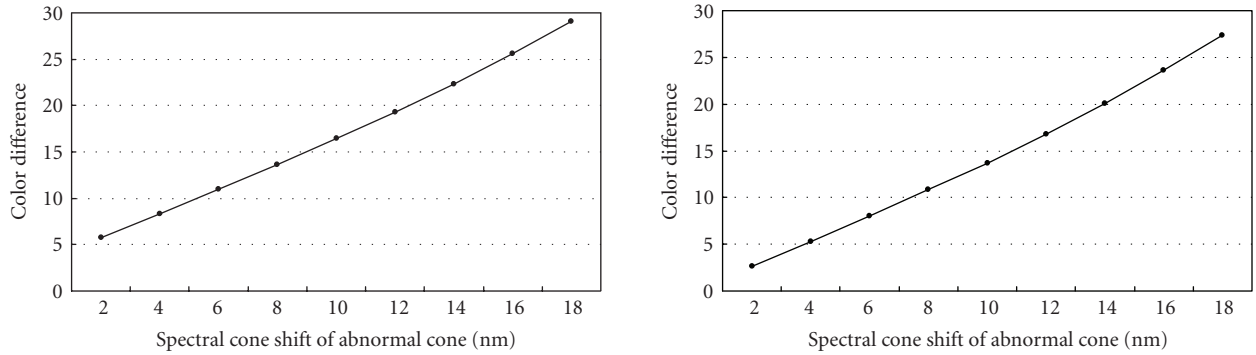

(a) Color difference for protan (b) Color difference for deutan

Figure 4: Color difference between normal trichromats and anomalous trichromats for the color caps in the CHT.

Table 1: The total error scores obtained with the CHT and FM100H test in normal subjects.

Age range (y)	Mean age (y)	No. of subjects	Total error score (mean ± std.)		P value
			CHT	FM100H	
10–19	16	28	17.3 ± 08.6	34.4 ± 24.6	<.05
20–29	24	10	17.9 ± 14.7	45.2 ± 21.1	<.05
30–39	32	6	28.4 ± 13.4	46.1 ± 20.2	<.05
40–49	46	14	30.1 ± 12.6	52.4 ± 19.2	<.05
50–59	57	19	31.0 ± 13.3	67.4 ± 18.6	<.05
60–69	63	12	34.8 ± 29.2	69.2 ± 32.5	<.05

In comparing the test reproducibility through the coefficient of variation, the CHT had a much higher reproducibility than the existing FM100H test. The TES of the normal subjects was relatively lower in the CHT that measured 31.5 ± 12.3 than in the FM100H test that measured 43.6 ± 16.2. In the subjects who have a CVD, the TES was higher in the CHT that measured 169.8 ± 40.2 than in the FM100H test that measured 157.3 ± 41.9. As seen in the above results, the CHT is more sensitive than the FM100H test since the CHT is performed on the monitor device that provides better color reproduction compared to the offline FM100H test. Furthermore, the coefficients of variation averaged 21.2% in the FM100H test and 9.1% in the CHT. These results mean that the CHT would be superior to the conventional FM100H test. However, the two tests showed a high correlation with a *Pearson* correlation coefficient of 0.965, meaning that the CHT would follow the basic principle of the conventional FM100H test. From the statistical analysis using the t test, the TES of the CHT also demonstrated a statistically significant increase when comparing subjects by age. The t test results showed a high confidence about the alternative hypothesis such as t value = 4.95, degree of freedom = 83, and P value = .001 that denotes the probability of obtaining a result at least as extreme as a given data point under the null hypothesis. The results of the TES of the CHT and the FM100H test in the color defective eyes of each age level are shown in Table 1. Both tests showed almost no statistical difference in all age groups, where the P value < .05, but rather showed a high correlation (*Pearson* correlation analysis: $r = 0.856$, Table 1). From the results, we see that the TES is significantly higher for the CHT than for the FM100T test. This is because the CHT would give more accurate and correct color reproduction than would the FM100H test.

The CHT has been also compared to a pseudoisochromatic plate test, the HRR test. The HRR test demonstrated 18 protan defectives showing a mild degree in 2, a medium degree in 7, and a severe degree in 9; 19 deutan defectives showing a medium degree in 4 and a severe degree in 15; 5 were unclassified subjects. The FM100H test showed 17 protan defectives, 21 deutan defectives, and 3 unclassified subjects, while the CHT showed 18 protan defectives, 19 deutan defectives, and 5 unclassified color defectives. As the severity of degrees in the HRR test was increased, the TES was increased in both the FM100H test and the CHT (Table 2).

The confusion lines used to determine the type of CVD have also been compared for the CHT and FM100H test. Generally, two confusion lines would be expected for a CVD [8]. Each line is represented by the range of confusing caps and their center. The primarily confusing caps for protan defectives ranged from the 22nd to 33rd caps at the center of the 26th cap and from the 64th to 72nd caps at the center of the 70th cap in the CHT, while they were ranged from the 15th to 16th caps at the center of the 17th cap and from the 58th to 68th caps at the center of the 64th cap in the FM100H test. And the primarily confusing caps for deutan defectives ranged from the 15th to 24th caps at the center of the 16th cap and from the 58th to 64th caps at the center of the 70 caps, while they ranged from the 12nd to 17th caps at the center of the 15th cap and from the 53th to 60th caps at the center of the 58th cap in the FM100H test. That is, the CHT

Table 2: The total error scores obtained with the CHT and FM100H test in three groups of subjects with color defects based on the HRR test.

Type of color defect (HRR test)	Total error score (mean ± std. dev.)		P value
	CHT	FM100H	
Mild	145.0 ± 59.5	91.0 ± 23.6	<.05
Moderate	153.6 ± 46.3	115.0 ± 15.6	<.05
Severe	171.8 ± 50.3	123.3 ± 23.3	<.05

Table 3: Position of the central caps characterizing the axis of confusion for color defective subjects on the CHT and FM100H test.

Type of color defect	CHT		FM100H	
	Central cap	Range	Central cap	Range
Protan	26	22–33	15	15–16
	70	64–72	64	58–68
Deutan	16	15–24	15	12–17
	58	58–64	58	53–60

would tend to express a more yellow-green-purple axis (Table 3).

To summarize, based on the outcome of these experiments, we can conclude that the CHT would work well as a color vision test by showing a high correlation with the FM100H test and it gives more elaborate, correct color reproduction than the FM100H test. For further research, we will look for crucial evidence that anomalous trichromats with bigger cone shift will be more defective in their color discrimination ability, particularly regarding a linear relationship.

5. CONCLUSIONS

In this paper, we have proposed a computerized color vision test for CVD. The CHT is a reproducible computer-based test that allows easy manipulation of test colors for the purposes of simulation and analysis of anomalies in color vision. The usefulness of the CHT was evaluated with both computer simulation and clinical experiments. The CHT is statistically consistent for all age groups with the FM100H test. A computer simulation was used to measure the variation of color defects according to spectral cone shift. From our simulation results, we can conclude that the anomalous trichromats are more defective in their color discrimination ability when the spectral cone shift is bigger. We could also see that the color gamut of the anomalous trichromats becomes smaller when the spectral cone shift increases. Another important conclusion through the simulation on the CHT is that color vision would be linearly degraded according to deficiency degree. Since the deficiency degree in the standardized CVD description is linearly measured, this observation is important for Part II of our study that aims at matching the error scores of the CHT to the standardized CVD description. Given the evidence, we can conclude that the CHT provides a reliable and quantitative measure of color defects. In Part II of the study, we discuss a color compensation scheme for anomalous trichromats. This color compensation scheme operates according to the deficiency degree standardized by the MPEG-21 multimedia framework.

REFERENCES

[1] D. McIntyre, *Color Blindness: Causes and Effects*, Dalton Publishing, Chester, UK, 2002.

[2] A. Vetro and C. Timmerer, "Digital item adaptation: overview of standardization and research activities," *IEEE Transactions on Multimedia*, vol. 7, no. 3, pp. 418–426, 2005.

[3] S. Yang, Y. M. Ro, J. Nam, J. Hong, S. Y. Choi, and J.-H. Lee, "Improving visual accessibility for color vision deficiency based on MPEG-21," *ETRI Journal*, vol. 26, no. 3, pp. 195–202, 2004.

[4] J. Birch, "Efficiency of the Ishihara test for identifying red-green colour deficiency," *Ophthalmic and Physiological Optics*, vol. 17, no. 5, pp. 403–408, 1997.

[5] D. V. de Alwis and C. H. Kon, "A new way to use the Ishihara test," *Journal of Neurology*, vol. 239, no. 8, pp. 451–454, 1992.

[6] I. H. Hardy, G. R. Rand, and C. Rittler, "HRR polychromatic plates," *Journal of the Optical Society of America*, vol. 44, no. 7, pp. 509–523, 1954.

[7] V. C. Smith, J. Pokorny, and A. S. Pass, "Color-axis determination on the Farnsworth-Munsell 100-hue test," *American Journal of Ophthalmology*, vol. 100, no. 1, pp. 176–182, 1985.

[8] G. Verriest, J. V. Laethem, and A. Uvijls, "A new assessment of the normal ranges of the Farnsworth-Munsell 100-hue test scores," *American Journal of Ophthalmology*, vol. 93, no. 5, pp. 635–642, 1982.

[9] S. J. Dain and J. Birch, "An averaging method for the interpretation of the Farnsworth-Munsell 100-Hue test—I. Congenital colour vision defects," *Ophthalmic and Physiological Optics*, vol. 7, no. 3, pp. 267–280, 1987.

[10] H. Jyrki, "A comparative study of several diagnostic tests of color vision used for congenital red-green defects," *Acta ophthalmologica. Supplement*, vol. 115, pp. 62–68, 1972.

[11] G. Verriest, J. Van Laethem, and A. Uvijls, "A new assessment of the normal ranges of the Farnsworth-Munsell 100-hue test scores," *American Journal of Ophthalmology*, vol. 93, no. 5, pp. 635–642, 1982.

[12] H. Cooper and A. Bener, "Application of a LaserJet printer to plot the Farnsworth-Munsell 100-hue color test," *Optometry and Vision Science*, vol. 67, no. 5, pp. 372–376, 1990.

[13] A. Linksz, "Color vision tests in clinical practice," *Transactions of the American Academy of Ophthalmology and Otolaryngology*, vol. 75, no. 5, pp. 1078–1090, 1971.

[14] V. C. Smith and J. Pokorny, "Spectral sensitivity of the foveal cone pigments between 400 and 700 nm," *Vision Research*, vol. 15, no. 2, pp. 161–171, 1975.

[15] J. Pokorny and V. C. Smith, "Evaluation of single-pigment shift model of anomalous trichromacy," *Journal of the Optical Society of America A*, vol. 67, no. 9, pp. 1196–1209, 1977.

[16] J. Pokorny, V. C. Smith, and I. Katz, "Derivation of the photopigment absorption spectra in anomalous trichromat," *Journal of the Optical Society of America A*, vol. 63, no. 2, pp. 232–237, 1973.

[17] P. DeMarco, J. Pokorny, and V. C. Smith, "Full-spectrum cone sensitivity functions for X-chromosome-linked anomalous trichromats," *Journal of the Optical Society of America A*, vol. 9, no. 9, pp. 1465–1476, 1992.

[18] M. Neitz and J. Neitz, "Molecular genetics of color vision and color vision defects," *Archives of Ophthalmology*, vol. 118, no. 5, pp. 691–700, 2000.

[19] A. Stockman and L. T. Sharpe, "The spectral sensitivities of the middle- and long-wavelength-sensitive cones derived from measurements in observers of known genotype," *Vision Research*, vol. 40, no. 13, pp. 1711–1737, 2000.

[20] L. T. Sharpe, A. Stockman, H. Jägle, et al., "Red, green, and red-green hybrid pigments in the human retina: correlations between deduced protein sequences and psychophysically measured spectral sensitivities," *The Journal of Neuroscience*, vol. 18, no. 23, pp. 10053–10069, 1998.

[21] G. Wyszecki and W. S. Stiles, *Color Science: Concepts and Methods, Quantitative Data and Formulae*, John Willey & Sons, New York, NY, USA, 2000.

[22] H. Brettel, F. Vienot, and J. D. Mollon, "Computerized simulation of color appearance for dichromats," *Journal of the Optical Society of America A*, vol. 14, no. 10, pp. 2647–2655, 1997.

[23] F. Vienot and H. Brettel, "Color display for dichromats," in *Color Imaging: Device-Independent Color, Color Hardcopy, and Graphic Arts VI*, vol. 4300 of *Proceedings of SPIE*, pp. 199–207, San Jose, Calif, USA, January 2000.

[24] C. Rigden, "The eye of the beholder designing for color-blind users," *British Telecommunications Engineering*, vol. 17, pp. 291–295, 1999.

[25] G. Kovács, I. Kucsera, G. Ábrahám, and K. Wenzel, "Enhancing color representation for anomalous trichromats on CRT monitors," *Color Research & Application*, vol. 26, no. 1, supplement, pp. 273–276, 2001.

[26] A. E. Krill and G. A. Fishman, "Acquired color vision defects," *Transactions of the American Academy of Ophthalmology and Otolaryngology*, vol. 75, no. 5, pp. 1095–1111, 1971.

Preliminary call for papers

The 2011 European Signal Processing Conference (EUSIPCO-2011) is the nineteenth in a series of conferences promoted by the European Association for Signal Processing (EURASIP, www.eurasip.org). This year edition will take place in Barcelona, capital city of Catalonia (Spain), and will be jointly organized by the Centre Tecnològic de Telecomunicacions de Catalunya (CTTC) and the Universitat Politècnica de Catalunya (UPC).

EUSIPCO-2011 will focus on key aspects of signal processing theory and applications as listed below. Acceptance of submissions will be based on quality, relevance and originality. Accepted papers will be published in the EUSIPCO proceedings and presented during the conference. Paper submissions, proposals for tutorials and proposals for special sessions are invited in, but not limited to, the following areas of interest.

Areas of Interest

- Audio and electro-acoustics.
- Design, implementation, and applications of signal processing systems.
- Multimedia signal processing and coding.
- Image and multidimensional signal processing.
- Signal detection and estimation.
- Sensor array and multi-channel signal processing.
- Sensor fusion in networked systems.
- Signal processing for communications.
- Medical imaging and image analysis.
- Non-stationary, non-linear and non-Gaussian signal processing.

Submissions

Procedures to submit a paper and proposals for special sessions and tutorials will be detailed at www.eusipco2011.org. Submitted papers must be camera-ready, no more than 5 pages long, and conforming to the standard specified on the EUSIPCO 2011 web site. First authors who are registered students can participate in the best student paper competition.

Important Deadlines:

Proposals for special sessions	15 Dec 2010
Proposals for tutorials	18 Feb 2011
Electronic submission of full papers	**21 Feb 2011**
Notification of acceptance	23 May 2011
Submission of camera-ready papers	6 Jun 2011

Webpage: www.eusipco2011.org

Organizing Committee

Honorary Chair
Miguel A. Lagunas (CTTC)

General Chair
Ana I. Pérez-Neira (UPC)

General Vice-Chair
Carles Antón-Haro (CTTC)

Technical Program Chair
Xavier Mestre (CTTC)

Technical Program Co-Chairs
Javier Hernando (UPC)
Montserrat Pardàs (UPC)

Plenary Talks
Ferran Marqués (UPC)
Yonina Eldar (Technion)

Special Sessions
Ignacio Santamaría (Unversidad de Cantabria)
Mats Bengtsson (KTH)

Finances
Montserrat Nájar (UPC)

Tutorials
Daniel P. Palomar (Hong Kong UST)
Beatrice Pesquet-Popescu (ENST)

Publicity
Stephan Pfletschinger (CTTC)
Mònica Navarro (CTTC)

Publications
Antonio Pascual (UPC)
Carles Fernández (CTTC)

Industrial Liaison & Exhibits
Angeliki Alexiou (University of Piraeus)
Albert Sitjà (CTTC)

International Liaison
Ju Liu (Shandong University-China)
Jinhong Yuan (UNSW-Australia)
Tamas Sziranyi (SZTAKI -Hungary)
Rich Stern (CMU-USA)
Ricardo L. de Queiroz (UNB-Brazil)

EURASIP
European Association for Signal Procesing

CTTC
Centre Tecnològic de Telecomunicacions de Catalunya

UPC